Journal of Mathematics and Informatics
Vol. 19, 2020, 115-123
ISSN: 2349-0632 (P), 2349-0640 (online)
Published 25 September 2020
www.researchmathsci.org
DOI: http://dx.doi.org/10.22457/jmi.v19a10182

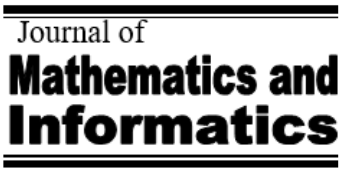

Multi-Focus Image Fusion Based on Non-Subsampled Shearlet Transform and Spiking Cortical Model

Wang Jing * **and** ***Zhang Gui-cang***

School of Mathematics & Statistics, Northwest Normal University
Gansu Lanzhou Province, 730070, China
*Corresponding author. Email: 1714986367@qq.com

Received 7 August 2020; accepted 19 September 2020

Abstract. In order to solve the problem of limited detail information retention in multi-focus image fusion algorithm, a multi-focus image fusion algorithm combining non-subsampled shearlet transform and Spiking cortical model is proposed. Firstly, the source image is decomposed by non-subsampled shearlet transform (NSST), Then the edge energy (EOE) is calculated and the low-frequency coefficients are fused by voting weighting method in the adaptive region; the high-frequency coefficients are fused by the Spiking cortical model (SCM) with the edge energy as the input. Finally, the fused image is obtained by inverse NSST. The experimental results show that the algorithm can retain more detailed information and has certain advantages in visual quality and objective evaluation.

Keywords: multi-focus image fusion；Non-subsampled shearlet transform；Spiking cortical mod- el； edge energy

AMS Mathematics Subject Classification (2010): 93A30, 00A71

1. Introduction

Image fusion is to effectively extract the complementary information associated with multiple sensors to obtain a comprehensive image with more abundant information [1]. Among them, multi- focus image fusion is an important branch in the field of image fusion Due to the limited depth of field of optical sensors, it is difficult to obtain an image with all the objects focused at the same time. Multi-focus image fusion can fuse multiple images with different focus points to get an image with clear focus [2]. At present, multi-focus image fusion has been widely used in digital photography, computer vision, target tracking monitoring and microscopic imaging Application prospect [3].

In recent years, Easley et al. [4] proposed a Non-subsampled shearlet transform

(NSST) with infinite decomposition directions NSST transform has good local time-frequency characteristics, multi direction and translation invariance. Therefore, the multi focus image fusion algorithm based on NSST transform can extract the edge texture and other details of the source image more effectively and achieve better fusion effect.

At present, region based fusion rules combine feature level fusion with pixel and fusion to achieve better fusion effect than other methods. Guo Di et al. Proposed an adaptive region by using the self similarity of a single image and the shared similarity between multi-source images. Because the block effect is easy to be produced by simple fusion rules at low frequency, this paper uses adaptive region to fuse low-frequency coefficients. SCM combines the advantages of PCNN [14] and ICM models, and according to the robustness of geometric changes, SCM can reduce the computational complexity In the field of image processing, in general spatial domain and transform domain algorithms, a single pixel is usually used to excite a single neural source in SCM. However, a single pixel can not achieve the goal, so edge energy (EOM) is used to excite SCM and fuse high frequency coefficients [5-7].

Therefore, this paper combines NSST transform, adaptive domain and SCM, and proposes a multi focus image fusion algorithm based on NSST adaptive region and SCM Secondly, according to the characteristics of low frequency and high frequency sub-band coefficients, edge energy (EOE) is calculated and low-frequency coefficients are fused by voting weighting method in adaptive region [12]; high-frequency coefficients are fused by SCM ignition map with edge energy as input; finally, NSST inverse transform is used to obtain fused image The simulation results show that the proposed algorithm can retain rich contour, detail and texture information, and improve the contrast and clarity of the fused image [13].

2. Related research

2.1. Spiking cortical model

The neurons in SCM are usually composed of three parts: receiving area, modulation area and Pulse emission area. The numerical expression of SCM model is as follows[6]:

$$F_{ij}(n) = s_{ij} \tag{1}$$

$$L_{ij}(n) = V_L \sum_{kl} W_{ijkl} Y(n-1) \tag{2}$$

$$U_{ij}(n) = fU(n-1) + s_{ij} \sum_{kl} W_{ijkl} Y_{kl}(n-1) + s_{ij} \tag{3}$$

$$E_{ij}(n) = gE_{ij}(n-1) + hY_{ij}(n-1) \tag{4}$$

$$Y_{ij}(n) = \begin{cases} 1, & if\ U_{ij}(n) > E_{ij}(n) \\ 0, & otherwise \end{cases} \tag{5}$$

In the receiving area, SCM neurons receive signals through two channels. One channel is the feed input s_{ij}. The other channel is the connection input L_{ij}. U_{ij} Is the dynamic threshold，Equation (5) indicates that，By comparison U_{ij} and E_{ij} .the pulse output of neurons is determined Y_{ij}. If the conditions of equation (5) are satisfied, the neuron will be activated and generate a pulse, which is characterized by $Y_{ij}=1$ or $Y_{ij}=0$. V_L is the magnitude scale term，W_{ijkl} is the connection，f and g is the attenuation coefficient, h is the threshold activity coefficient.

The setting of iteration times n has a great influence on the calculation cost and the final fusion effect. A time matrix model with the same size as the source image is used to record the firing information of neurons. The expression of time matrix is shown in equation (6).

$$T_{ij}^{kl}(n)=T_{ij}^{kl}(n-1)+Y_{ij}^{kl}(n) \tag{6}$$

where T is the time matrix. According to the gray distribution of the image pixels, the iteration number n can be adaptively determined.

2.2. Non-subsampled shearlet transform

NSST is divided into two steps: the first step is to decompose the multi-focus source image in l-level to obtain the low-frequency and high-frequency sub-band coefficients; the second is to decompose the image in multi-scale and multi-direction through the improved shearlet filter bank (SFB) [7]. In fact, the coarse multi-scale decomposition image can be obtained by using non- sub-sampled pyramid filter (NSPF). That is to say, the source image is decomposed in l-level and k-direction to obtain the coefficient with the same size as the source image[10]. At that time, it represents the low-frequency coefficient and the high-frequency coefficient $C^{kl}(r)$. When $l=0$, it means low frequency coefficient, when $l>0$, it means high frequency coefficient Fig. 1 is a schematic diagram of the two-stage NSST decomposition [11].

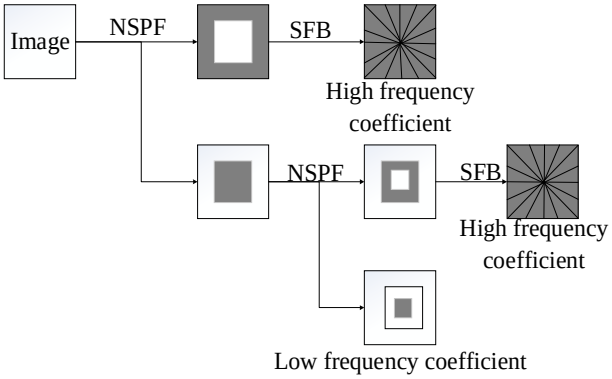

Figure 1: NSST decomposition diagram

3. Realization of image fusion algorithm

The image fusion algorithm is described as follows: source images f^A and f^B are two

matched images with different focal points respectively, F_r is the fused image.

Firstly, NSST is used to decompose source image f^A and f^B to obtain coefficients $C_A^{kl}(r)$ and $C_B^{kl}(r)$, respectively.

Secondly, the edge energy at pixel r is calculated.

$$EOE(r)=\left[E_1\cdot C^{kl}(r)\right]^2+\left[E_2\cdot C^{kl}(r)\right]^2+\left[E_3\cdot C^{kl}(r)\right]^2 \tag{7}$$

where， $r\in(i,j)$， E_1、E_2、E_3 are:

$$E_1=\begin{bmatrix}-1&-1&-1\\2&2&2\\-1&-1&-1\end{bmatrix}\quad E_2=\begin{bmatrix}-1&2&-1\\-1&2&-1\\-1&2&-1\end{bmatrix}\quad E_1=\begin{bmatrix}-1&0&-1\\0&4&0\\-1&0&-1\end{bmatrix} \tag{8}$$

3.1. low frequency coefficient fusion

f_{low}^A and f_{low}^B are the low-frequency coefficients of source image f^A and f^B after NSST decomposition, and each adaptive region is measured by edge energy. If the edge energy of f_{low}^A is larger than that of f_{low}^A in an adaptive region, then all pixels in $\gamma\in L_w^s(r)$ will get one vote in this adaptive region of f_{low}^A, that is:

$$v^A(\gamma)=v^A(\gamma)+1\ ,\ \ \gamma\in L_w^s(r) \tag{9}$$

where $v^A(\gamma)$ is the counter at spatial position γ. The initial values of $v^A(\gamma)$ and $v^B(\gamma)$ are 0. After all adaptive regions are compared, the counting stops. The number of counter times $v^A(\gamma)$ and $v^B(\gamma)$ with the same size as the source image are obtained.In the following, $v^A(\gamma)$ and $v^B(\gamma)$ are used to represent the last vote number of γ pixel at location.Finally, the weighted method is used to construct pixels.

$$f_{low}^F(r)=\frac{v^A(r)}{v^A(r)+v^B(r)}f_{low}^A(r)+\frac{v^B(r)}{v^A(r)+v^B(r)}f_{low}^B(r) \tag{10}$$

3.2. High frequency full integration

For the decomposed high frequency coefficients $C_A^{kl}(r)$ and $C_B^{kl}(r)\ (l>0)$， EOE and SCM are combined. f_{high}^F is the high frequency coefficient of the fused image.

$$s_{ij}=\sum_{r\in D}w(r)EOE(r) \tag{11}$$

where $w(r)$ is the weighting factor， D is the neighborhood window centered on pixel r.

Then the high frequency coefficients of the fused image are selected by pulse synchronization.Calculate the total ignition times $T_{ij}^{kl}(n)=T_{ij}^{kl}(n-1)+Y_{ij}^{kl}(n)$ of each high frequency coefficient.After N iterations, the high frequency coefficient of fusion is determined by equation (12).

$$C_F^{kl}=\begin{cases}C_A^{kl}\ ,\ if\ \mathrm{TR}_A^{kl}(r)\geq\mathrm{TR}_B^{kl}(r)\\C_B^{kl}\ ,\ if\ \mathrm{TR}_A^{kl}(r)<\mathrm{TR}_B^{kl}(r)\end{cases} \tag{12}$$

where $TR_A^{kl}(r)$ and $TR_B^{kl}(r)$ are the total number of local ignition respectively, and the calculation formula is as follows:

$$TR^{kl}(r)=\sum_{k,l\in D}T^{kl}(r) \tag{13}$$

Finally, the fused image F_r is reconstructed by inverse NSST transform using the fused low frequency coefficient f_{low}^{F} and high frequency coefficient f_{high}^{F}. the block diagram of the proposed fusion algorithm is shown in Fig. 2.

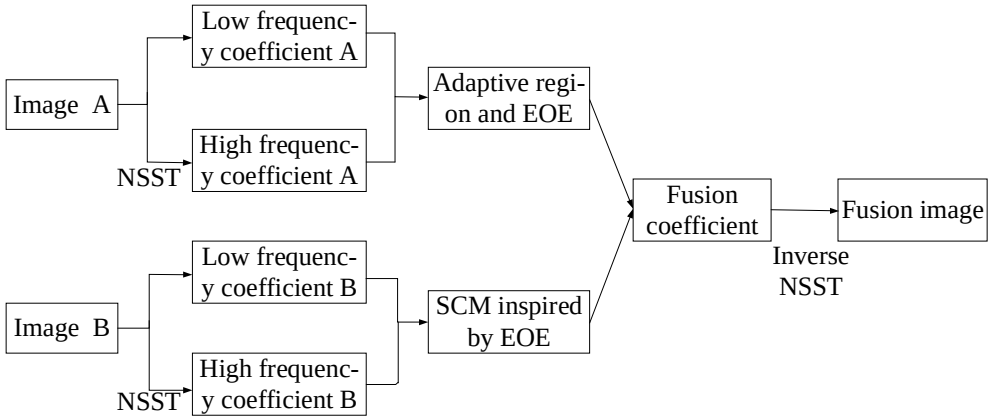

Figure 2: Block diagram of multi-focus image fusion algorithm based on NSST adaptive region and SCM

4. Experimental results and analysis

In order to evaluate the performance of the proposed fusion algorithm, we use some multi-focus images to test the visual appearance and objective standards. The fusion algorithm based on NSCT_PCNN (NSCT_PCNN), the fusion algorithm based on SCM and definition (SCM_SF), the fusion algorithm based on NSCT and improved PCNN (NSCT_IPCNN) are all the comparative algorithms in this paper. Mutual information MI, edge strength $Q^{AB/F}$ were used as objective evaluation criteria. Among them, MI can calculate how much information of the source image is moved to the fused image [8]; $Q^{AB/F}$ can measure how much edge information is moved from the source image to the image fusion [9].

In Fig 3，two pairs of images with strict registration and size are 256×256 tested by Matlab (2016a).

(a) (b) (c) (d)

Figure 3: Multi-focus image experimental pair. (a)“Pepsi” Left; (b)“Pepsi ”Right; (c)“Clock” Left; (d)“Clock” Right;

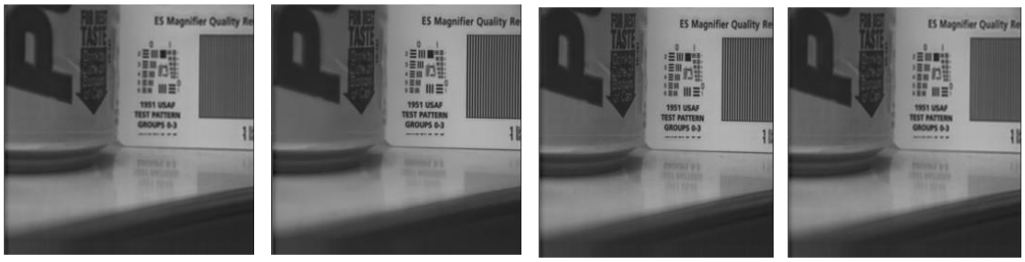

(e) (f) (g) (h)

Figure 4: Results of four algorithms of “Pepsi”. (e) NSCT_PCNN; (f) SCM_SF; (g) NSCT_IPCNN; (h) Algorithm in this paper.

Figure 4 to figure 5 show the fusion effect of different algorithms for four groups of images. From the experimental results, it is not difficult to find that different algorithms have different effects on different images. Below we will elaborate from subjective and objective two angles.

From a subjective point of view, different algorithms can display a lot of details in Figure 4, but the difference is that, compared with the other three algorithms, the algorithm in this paper makes a more accurate judgment on the focused image, which greatly improves the details, vision and clarity of the fused image; image e is relatively fuzzy and has low brightness in detail; the brightness of figure f is improved; and the image quality is improved; Image G is improved in detail texture, but some noise is introduced into the fusion result, which makes the image not clear enough; therefore, the fusion effect of graph h is better than other algorithms.

(i) (j) (p) (q)

Figure 4: Results of four algorithms of “Clock” (i) NSCT_PCNN ; (j) SCM_SF; (p) NSCT_IPCNN; (q) Algorithm in this paper.

From a subjective point of view, the four algorithms in Fig. 4 (i) to figure (q) can achieve a certain fusion effect. The comparative study shows that the brightness of figure i is slightly lower; the brightness of figure j is improved, but the detail texture information is low; although the edge information of the fused image can be clearly seen in Figure p, the letters in the clock and the letter "3M" on the table are not clear; The quality of books on shelf, letters on clock and books on desk are easy to observe. This shows that the algorithm can effectively improve the clarity of the fused image, improve the ability to display details and textures, and achieve better fusion effect.

Table 1: Objective evaluation of "Pepsi" image fusion results

Fusion algorithm	$Q^{AB/F}$	MI	Time(S)
NSCT_PCNN	0.68	7.49	974.3
SCM_SF	0.70	6.89	809.9
NSCT_IPCNN	0.72	8.08	558.2
The algorithm in this paper	**0.79**	**7.81**	**308.3**

Table 2: Objective evaluation of "Clock" image fusion results

Fusion algorithm	$Q^{AB/F}$	MI	Time(S)
NSCT_PCNN	0.71	6.35	687.0
SCM_SF	0.74	5.54	520.4
NSCT_IPCNN	0.78	7.75	392.2
The algorithm in this paper	**0.82**	**7.81**	**238.9**

It can be seen from table 1 and table 2 that the algorithm in this paper has the highest $Q^{AB/F}$. it also has a good performance in mutual information. In the running time, the algorithm is compared with the traditional NSCT_ PCNN is much shorter than NSCT_ IPCNN and SCM_ Compared with SF, the proposed algorithm has a great improvement in $Q^{AB/F}$, MI and running time, good results have been obtained.

5. Concluding remarks

This paper proposes a multi-focus image fusion algorithm combining non-subsampled shearlet transform and Spiking cortical model. In the frequency domain, the edge energy and adaptive region fusion algorithm is used, and the high frequency coefficients are fused with SCM ignited by edge energy, so as to improve the clarity and spatial characteristics of the fused image.

Fund Project

1) National Natural Science Foundation of China: (Project Number: 61861040)
2) Gansu Province Science and Technology Project Funding: (Project Number: NO.17YF1FA119)
3) Lanzhou Science and Technology Plan Project: (Project Number: 2018-4-35)
4) Gansu Provincial Department of Education Science and Technology Achievements Transformation Project: (Project Number: 2017D-09).

Acknowledgement. The authors are grateful to the reviewers for their valuable comments for improvement of the paper.

REFERENCES

1. R.S.Blum and Z.Liu, *Multi-Sensor Image Fusion and its Applications*, CRC Press, Boca Raton, (2005) 1-10.
2. L.Wei and W.Zeng-fu, A novel multi-focus im- age fusion method using multi-scale shearing non-local guided averaging filter, *Signal Processing*,, 166 (2020) 1-24.
3. A.Goshtasby and S.G.Nikolov, Guest editorial, Image fusion: advances in the state of the art, *Information. Fusion*, 8(2) (2017) 114-118.
4. Glenn Easley, Demetrio Labate and Wang-Q. Lim, Sparse directional image representations using the discrete shearlet transform, *Applied and Computational Harmonic Analysis*, 25 (2008) 25- 46.
5. Liu Shengpeng and Fang Yong, Fusion algorithm based on contourlet transform and ipcnn and its application in visible and infrared image fusion, *Journal of Infrared and Millimeter Wave*, 26(3) (2007) 217-221.
6. Zhao Jie, Wenxin, Liu shuaiqi, et al., Multi focus image fusion based on NSST adaptive region and SCM, *Computer Science*, 44(3) (2017) 318-322.
7. Liu Xing-bin, Mei Wen-bo and Du Hui-qian, Structure tensor and non-sub-sampled shearlet transform based algorithm for CT and MRI image fusion, *Neurocomputing*, 235 (2017) 131-139.
8. Yang Bin and Li Shu-tao, Multi-focus image fusion and restoration with sparse representation, *IEEE Trans. On Instrumentation and Measurement*, 59(4) (2010) 884–892.
9. Wang Rui and Du Lin-feng, Infrared and visible image fusion based on random projection and spare representation, *International Journal Remote Sensing*, 35 (2014) 1640-1652.
10. Yin Ming, Liu Xiao-ning, Liu Yu, et al., Medical image fusion with parameter-adaptive pulse coupled-neural network in non-subsampled shearlet transform domain, *IEEE Transaction on Instrumentation and Measurement*, 68 (1) (2019) 49-64.
11. Yang Yong, Wan Wei-guo, Huang Shu-ying, et al., Multi-focus image fusion based on sparse representation and non-subsampling shearlet transformation, *Minicomputer System*, 38(2) (2017) 386-392.
12. Wang Jing,Zhang, Guicang and Su Jinfeng, Medical image fusion combining singular value decomposition and mean gradient, *Journal of Mathematics and Informatics*, 17 (2019) 31-54.
13. Jinhui Gong, Guicang Zhang and Kai Wang, Human iris localization combined with ant colony and improved hough circle detection, *Journal of Mathematics and*

Informatics, 16 (2019) 23-39.

14. Li Hongjie, Zhang Guicang and Zhu Zongyuan, Color image segmentation based on PCNN, *Journal of Mathematics and Informatics*, (13) (2018) 41-53.